



HOKKAIDO UNIVERSITY

Title	Structural change in non-fractal particle clusters under fluid stress
Author(s)	Harada, S. ; Tanaka, R. ; Nogami, H. et al.
Citation	Colloids and Surfaces A Physicochemical and Engineering Aspects, 302(1-3), 396-402 https://doi.org/10.1016/j.colsurfa.2007.03.003
Issue Date	2007-07-20
Doc URL	https://hdl.handle.net/2115/28015
Type	journal article
File Information	CSPEA302-1-3.pdf



Structural Change in Non-Fractal Particle Clusters under Fluid Stress

S. Harada[†], R. Tanaka[†], H. Nogami[‡], M. Sawada[‡] and K. Asakura[†]

[†] *Div. of Field Engineering for Environment, Graduate School of Eng., Hokkaido Univ.
N13-W8, Sapporo 060-8628, Japan*

[‡] *Murata Manufacturing Company, Ltd.,
10-1, Higashi Kotari 1-chome, Nagaokakyo, Kyoto 617-8555, Japan*

Corresponding Author : Shusaku Harada
Address : Division of Field Engineering for Environment,
Graduate School of Engineering, Hokkaido University
N13-W8, Sapporo 060-8628, Japan
Tel/Fax : +81-11-706-6310
E-mail : harada@eng.hokudai.ac.jp

Abstract

The restructuring of particle clusters having a dense packing structure under fluid stress is investigated numerically. The rearrangement of particles in the cluster and the breakage of their interparticle bonds in simple shear flow are examined by the Lagrangian-type simulation. The hydrodynamic force exerted on multiple particles is estimated by Stokesian dynamics approach. The interparticle force is calculated from the retarded van der Waals potential based on the Lifshitz theory. The simulation results show that the particle cluster rotates with the rotation of the surrounding flow and deforms due to the fluid stress along the principal axes of the stress tensor. These complex effects bring the irreversible change of the internal structure to the cluster. It is found that the structural change of the cluster can be explained by the initial rearrangement of primary particles and the successive crack growth that takes a long time. Such a long-term structural change is analogous to that of the fatigue crack growth of solid materials. We discuss the dynamics of the restructuring of a dense cluster from this point of view and propose a mathematical model which describes the restructuring process in a flow field.

Keywords : particle cluster; breakup; shear flow; numerical analysis; restructuring; Stokesian dynamics

Introduction

The dispersion process of particle clusters suspended in a fluid is important for various applications in industrial fields. For example, the dispersion state of particle affects the rheological properties of the suspension. Also, it plays a key role in handling of micro- and nano particles such as the fabrication of the ordered assemblies [1].

The aggregation and the fragmentation of particle clusters in fluid flow have been studied in the fields related to colloidal science [2]. In the previous studies, population balance models have been developed for predicting the size distribution of particle clusters [3]. The population balance approaches are based on “addition” and “division” of particle clusters. That is, the clusters collide and unite in the motion of surrounding flow with a certain frequency. On the other hand, the clusters are divided into small pieces by fluid stress at a certain rate. By modeling these fluid effects, one can predict the size distribution of clusters in global scales.

In the population balance model, some parameters are required for representing loss and growth of the clusters. They are usually defined as functions of the size and the parameters related to the structure of the cluster such as the interparticle connectivity and the space-filling property as explained below. However, it is difficult to determine the parameters precisely because the actual effect of the surrounding flow on the cluster is more complicated. The fluid flow deforms, warps, entangles and disentangles the clusters. Consequently the clusters change their internal structures. In other words, not only does the fluid flow immediately contribute to “addition” and “division” of the particle clusters, but also it affects their loss and growth rates. For quantitative prediction of the dispersion state of particles in fluid, the detailed understanding of such complicated effects of the surrounding flow has been required. However, even the restructuring kinetics of an isolated cluster has not been understood satisfactorily.

The restructuring of particle cluster can be frequently found especially in shear flow. This is because shear flow consists of both the rotation and the extension of fluid, and this combination brings about the peculiar motion of immersed objects. The motion of particle clusters in shear flow has been interesting not only in colloidal science but in various fields such as fluid dynamics [4] and polymer science [5].

In the field of colloidal science, the restructuring of particle clusters has been often reported from a viewpoint of the change in space-filling properties[6]-[8]. Generally the space-filling properties of clusters are expressed by the fractal dimension and it is close to 3 if the cluster has a compact shape [2]. However, in case of non-fractal particle cluster, the internal connectivity could be

changed with its fractal dimension kept constant. Recently authors have studied the restructuring of a non-fractal particle cluster in shear flow by numerical simulation [9]. We demonstrated that a loose non-fractal cluster increases the coordination number and it turns into a dense cluster owing to the fluid stress. That is, the fluid stress brings about the rearrangement of primary particles and consequently the interparticle connectivity changes inside the cluster.

The purpose of this study is to understand the structural change of a non-fractal particle cluster under fluid stress, *i.e.*, the change in the interparticle connectivity due to the surrounding flow. We examined the dynamic behavior of a particle cluster in shear flow by Lagrangian particle simulation. There have been some numerical studies on the dynamics of a particle cluster in a flow field by using fluid force models [10]-[12]. However, the accurate estimations of both the short- and the long-range hydrodynamic interaction of particles are required for the quantitative understanding of the structural change of cluster. Thus we adopted the Stokesian dynamics approach for the calculation of hydrodynamic effect of surrounding flow. In this study, we focus on the mechanism of the restructuring of a dense particle cluster and discuss its influence on the fragmentation process.

Numerical Methods

The motion of an isolated particle cluster in simple shear flow is simulated by Stokesian dynamics approach. The basic equations and the numerical scheme are similar to the original Stokesian dynamics analysis [13]. On the assumption that the inertias of both particle and fluid are adequately small, the mobility matrix of particle is derived from multipole expansion of Oseen tensor in Stokes flow and Faxen's law. By the mobility matrix, the external force, torque, and the stresslet are related to the particle velocity, angular velocity and the rate of strain tensor of the undisturbed flow field. The grand mobility matrix \mathbf{M} , which describes the mobility of all particles, is inverted and \mathbf{M}^{-1} is divided in the following components.

$$\begin{pmatrix} \mathbf{F} \\ \mathbf{T} \\ \mathbf{S} \end{pmatrix} = \mathbf{M}^{-1} \begin{pmatrix} \mathbf{U} - \mathbf{u}^\infty \\ \boldsymbol{\Omega} - \boldsymbol{\Omega}^\infty \\ -\mathbf{E}^\infty \end{pmatrix}, \quad (1)$$

$$\mathbf{M}^{-1} = \begin{pmatrix} \mathbf{R}_{FU} & \mathbf{R}_{F\Omega} & \mathbf{R}_{FE} \\ \mathbf{R}_{TU} & \mathbf{R}_{T\Omega} & \mathbf{R}_{TE} \\ \mathbf{R}_{SU} & \mathbf{R}_{S\Omega} & \mathbf{R}_{SE} \end{pmatrix}, \quad (2)$$

where \mathbf{F} , \mathbf{T} and \mathbf{S} are the external force, torque acting on all particles and the stresslet, \mathbf{U} and $\boldsymbol{\Omega}$ are the particle velocity and the rotational velocity, \mathbf{u}^∞ , $\boldsymbol{\Omega}^\infty$ and \mathbf{E}^∞ are the flow velocity, rotational

velocity and the rate of strain tensor respectively. $\mathbf{R}_{FU}, \mathbf{R}_{F\Omega}, \dots$ indicate the component resistance matrices of \mathbf{M} . The full description of the grand mobility matrix \mathbf{M} can be found in the article by Durlafsky *et al.*[14].

From Eqs.(1) and (2), the velocity and the angular velocity of individual particles are calculated as follows;

$$\begin{pmatrix} \mathbf{U} \\ \mathbf{\Omega} \end{pmatrix} = \begin{pmatrix} \mathbf{u}^\infty \\ \mathbf{\Omega}^\infty \end{pmatrix} + \begin{pmatrix} \bar{\mathbf{R}}_{FU} & \bar{\mathbf{R}}_{F\Omega} \\ \bar{\mathbf{R}}_{TU} & \bar{\mathbf{R}}_{T\Omega} \end{pmatrix}^{-1} \left[\begin{pmatrix} \mathbf{F} \\ \mathbf{T} \end{pmatrix} + \begin{pmatrix} \bar{\mathbf{R}}_{FE} \\ \bar{\mathbf{R}}_{TE} \end{pmatrix} : \mathbf{E}^\infty \right], \quad (3)$$

where $\bar{\mathbf{R}}$ is the modified resistance matrix taking lubrication effect into consideration and is calculated as

$$\bar{\mathbf{R}} = \mathbf{R} + \mathbf{R}_{2B} - \mathbf{M}_{2B}^{-1}, \quad (4)$$

where \mathbf{R}_{2B} is the resistance matrix for a pair of particles [15, 16]. \mathbf{M}_{2B} is the pair mobility matrix calculated in a similar way to the grand mobility matrix \mathbf{M} . The instantaneous position of particles is calculated by numerical integration of Eq.(3).

The surrounding flow field is simple shear flow and is expressed as follows;

$$\mathbf{u}^\infty(\mathbf{r}) = \mathbf{\Omega}^\infty \times \mathbf{r} + \mathbf{E}^\infty \cdot \mathbf{r}, \quad (5)$$

where

$$\mathbf{\Omega}^\infty = -\frac{\dot{\gamma}}{2} \begin{pmatrix} 0 \\ 0 \\ 1 \end{pmatrix}, \quad \mathbf{E}^\infty = \frac{\dot{\gamma}}{2} \begin{pmatrix} 0 & 1 & 0 \\ 1 & 0 & 0 \\ 0 & 0 & 0 \end{pmatrix} \quad (6)$$

and $\dot{\gamma}$ is shear rate. The schematic diagram and the coordinate system of the simulation are shown in Fig.1. From Eq.(6), one can easily find that a simple shear flow consists of pure rotation with angular velocity $\dot{\gamma}/2$ and also planar extension along $y = x$ and compression along $y = -x$ with strength $\dot{\gamma}/2$ respectively.

As also shown in Fig.1, the particle cluster used here is dense random packing of one hundred primary particles having a non-fractal structure. The fractal dimension Fr , which expresses the space-filling property of cluster, is set to 3.0. The average coordination number for the initial condition k_0 is 5.54. Generally, the coordination number expresses the density of the contact-network among particles in the system of granular materials. In this study, the average coordination number is defined by the average number of particles existing within 2nm from each particle. k_0 is somewhat less than the well-known value of dense random packing of spherical particles ($k = 6.0 \sim 8.0$). This is because the particle cluster used here consists of only a hundred primary particles, and consequently the number of particles near the cluster surface, which cannot bond the neighboring particles sufficiently, is comparable with the total number of particles.

The primary particle is assumed to be a perfectly smooth sphere with the diameter $2a = 650\text{nm}$. For the physical properties of particle and fluid, those of polystyrene and ethanol are used. The particle and the fluid density are $\rho_p = 1056\text{kg/m}^3$, $\rho_f = 790\text{ kg/m}^3$ respectively and the fluid viscosity is $\mu = 1.2 \times 10^{-3}\text{ Pa}\cdot\text{s}$. The interparticle force is calculated from the retarded van der Waals potential. The potential is calculated by the rigorous approach which is the combination of retarded Hamaker constant based on Lihshitz theory and a Hamaker geometrical factor [17, 18]. The corresponding non-retarded Hamaker constant is $A = 9.68 \times 10^{-21}\text{J}$. The Brownian perturbation force is neglected on the assumption of large Péclet number $Pe = 6\pi\mu a^3\dot{\gamma}/k_B T$. (k_B : Boltzmann constant, T : temperature). In this simulation, $Pe > O(10^3)$ is satisfied for all conditions for the temperature $T = 300\text{K}$.

The assumption that both the particle and fluid inertia can be neglected is reasonable on the condition that the dimensionless parameters $Re = \rho_f a U / \mu$ and $St = \rho_p a U / \mu$ are less than unity. Where U is the characteristic velocity and is defined by both $U = A / 6\pi\mu a^2$ (the characteristic velocity of the response to the interparticle force) and $U = a\dot{\gamma}$ (the characteristic velocity of surrounding flow). The parameters defined by the former U adequately satisfy $Re, St \ll 1$ for given fluid and particle properties. In addition, we set the shear rate so as to satisfy $Re, St \ll 1$ defined by the latter U .

In the simulation, if the distance between particles is closer than the contact distance $\delta = 1\text{ nm}$, van der Waals force acting on them is set equal to zero and any repulsive force is not given them. Owing to lubrication effect, any overlap of particles (*i.e.*, the distance between the centers of the particle $r < 2a$) does not occur in this simulation. The contact distance used here seems to be greater because it is generally considered as the several angstroms [19, 20]. In angstrom lengthscales, there are various complex effects caused by the molecular nature of the surrounding fluid *i.e.*, the structural force, the lubrication effect at molecular scale and also the Brownian effect, are significant. In this study, we ignored these microscopic effects so as to focus on the particle dynamics for a given interparticle force.

The verification of the simulation method, the calculation condition such as time step, and the further discussions on the assumptions used here can be found in our previous article [9].

Results and discussion

Structural change of non-fractal cluster

Figure 2 shows the dynamic behavior of a non-fractal particle cluster in shear flow for $\mu\dot{\gamma}=23.9\text{Pa}$. The black arrows in the figure illustrate the rotational motion of the cluster, while the gray ones illustrate the translational motion. As shown in Fig.2, the particle cluster initially rotates like a rigid body with the rotation of flow (Fig.2(b)) and slightly translates in x direction owing to its asymmetric configuration (Fig.2(b)-(d)). The rotation speed of the cluster is almost identical with that of the flow (the nondimensional time per a rotation $\dot{\gamma}t = 4\pi$). After the cluster rotates rigidly for a very long time (approximately a hundred rotations), it begins to deform irreversibly (Fig.2(f)-(h)). Finally, the cluster ruptures and divides into two child clusters (Fig.2(i)).

In our previous study [9], the fragmentation process of loose particle clusters which have different space-filling properties was examined by the same simulation method. We showed that the structural change before rupture plays a significant role on the fragmentation process of loose clusters having high fractal dimensions. However, such a long-term structural change of dense clusters as shown here was not observed in the case of loose clusters. Therefore, this behavior is peculiar to dense packing clusters.

Long-term growth of cracks in clusters

In order to investigate the long-term deformation of the dense cluster as shown in Fig.2, we here examine the change in the internal structure of the cluster before rupture. Figure 3 shows the relation between the nondimensional time $\dot{\gamma}t$ and the average coordination number k for $\mu\dot{\gamma}=23.9\text{Pa}$. It is found that the change in the coordination number is divided into three characteristic stages, that is, (I) rapid change from the initial coordination number to the stable one, (II) slow decrease over a long period of time and (III) rapid and irregular decrease toward the rupture.

The inset of Fig.3 is a close-up of the change in the average coordination number at an early stage. As shown in the inset, the stage I is short and corresponds to the period that the cluster rotates one or a few times. In contrast, the stage II is surprisingly long. Throughout the stage II, the coordination number decreases irreversibly with the fluctuation. The amplitude of the fluctuation keeps almost constant value and it seems to be synchronized with the rotation of the cluster (See also Fig.5. Because the cluster experiences twice compression/expansion per a rotation, the fluctuation period is almost $\dot{\gamma}t = 2\pi$). This fluctuation of the coordination number can be interpreted as the periodic structural change in the cluster as a result of periodic passages through the principal axes of the stress tensor due to the rotation of the cluster. On the other hand,

the irreversible change of the coordination number implies that flaws (cracks) increase gradually in the particle cluster.

Figure 4 shows the change in the average coordination number of the particle cluster for various fluid stresses $\mu\dot{\gamma}$. The inset of the figure indicates the coordination number at early stages for some conditions. The initial structure of the cluster is common and the initial coordination number k_0 is 5.54 for all conditions. Figure 4 indicates that there are similarities between the changes in the coordination number for all $\mu\dot{\gamma}$. As mentioned above, they can be divided into three stages. Initially the coordination number reaches the respective stable values (k_S) by the time the cluster rotates a few times (stage I). The inset of the figure shows that the stable coordination number k_S decreases with increasing $\mu\dot{\gamma}$. This reason is explained as follows. The larger fluid stress enlarges the periodic deformation of the cluster which occurs during the stage II. Consequently, the connectivity in the particle cluster decreases for larger applied stress $\mu\dot{\gamma}$ since the cluster requires the larger mobility for such a short-term periodic deformation. Therefore the stage I can be interpreted as the transition period from the initial structure to the possible structure being subjected to the periodic deformation. The latter structure consists of various probable configurations under the applied flow field.

After the coordination number reaches the stable one, it decreases linearly (stage II). The slope of the decrease in the coordination number is more abrupt for larger $\mu\dot{\gamma}$. During this stage, the cluster rotates like a rigid body for small $\mu\dot{\gamma}$ or rotates with the periodic deformation for large $\mu\dot{\gamma}$. However the irreversible change in the structure occurs by degrees and flaws increase inside the cluster. After a while, the coordination number decreases rapidly (stage III) and finally the cluster ruptures in all cases.

Here we examine the dependence of the stable coordination number k_S on the cluster structure. Figure 5 shows the coordination number k in clusters having different initial structures at an early stage. The solid line indicates the cluster for initial coordination number $k_0 = 5.54$ and the dashed line indicates the cluster having a rather loose structure for $k_0 = 5.04$. As shown in Fig.5, the coordination numbers of primary particle in both clusters reach the similar values. As mentioned above, the initial rearrangement of primary particles is interpreted as the structural change from the initial structure to that suitable for the periodic deformation. It is found from Fig.5 that the stable coordination number k_S , which allows the periodic deformation of cluster for respective fluid

stresses $\mu\dot{\gamma}$, is not dependent on the initial structure and it is determined only by the condition of the surrounding flow.

Scaling of long-term deformation of cluster

In this section, we discuss the mechanism of the long-term deformation of dense particle clusters shown above. The deformation of the cluster arises from the breakage of interparticle bonds and it is determined by a balance between the strength of clusters resulting from the interparticle force and the fluid stress acting on the cluster. In the previous studies, Fragmentation number Fa was used for characterizing the fragmentation process of particle clusters in fluid flow [2]. It is defined as the ratio of the fluid stress to the cohesive strength H and $Fa = \mu\dot{\gamma}/H$. Here we consider the characteristic cohesive strength $H = A/a^3$ (the characteristic inter-particle force A/a divided by the characteristic cross-sectional area a^2) and define $Fa = \mu\dot{\gamma}a^3/A$ in the simplest way, and discuss the long-term deformation of the particle cluster by the fragmentation number Fa .

Figure 6 shows the relationship between the coordination number $k - k_S$ and the scaled time. As shown in the figure, the decrease of the coordination number is well scaled with a nondimensional time $Fa^{2.5}\dot{\gamma}t$. Since $k - k_S$ indicates the decrease of the coordination number from the stable one, $-(k - k_S)$ can be interpreted as the amount of the flaw in the particle cluster. The solid line indicates the fitting exponential function $k - k_S = C \exp(\lambda Fa^{2.5}\dot{\gamma}t)$, where C and λ are the fitting constants and $C = -0.05$ and $\lambda = 2.5 \times 10^{-8}$ respectively. This exponential function is the solution of the following differential equation;

$$\frac{d(k - k_S)}{d(\dot{\gamma}t)} = \lambda Fa^{2.5} (k - k_S). \quad (7)$$

The form of Eq.(7) is identical with that of the simplest population balance equation. That is, the rate of the flaw increase (the decrease in the number of the interparticle bond per unit time) is proportional to the instantaneous amount of the flaw in the cluster. This equation implies that the increase of the flaw weakens the strength of the particle cluster as time passes.

The well-known theory on the strength of particle agglomerates was developed by Rumpf [21]. In his theory, the strength of the agglomerate is considered as the mean cohesive force caused by the interparticle force per a fragmentation area. On the other hand, Kendall [22] derived the agglomerate strength based on the fracture mechanics. In Kendall's theory, the particle agglomerate is considered as a solid body which satisfies the Griffith energy criterion of fracture, and the strength is calculated by a fracture model based on the crack growth in the agglomerate.

Here we suggest one possible interpretation of the the flaw increase as shown in Fig.6 by the similar approach to Kendall's theory, that is, the analogy to the crack growth in solid materials. In the material science, the fatigue crack growth under cyclic load is expressed as Paris law [23] and is given by

$$\frac{dc}{dN} \sim (\Delta K)^m \quad (8)$$

where c is the crack length, N is the number of cycles. ΔK is the differential stress intensity factor $K_{\max} - K_{\min}$ where K_{\min} , K_{\max} are the minimum and maximum stress intensity factors during the cyclic load. m is the parameter and is generally $2 \sim 4$. The stress intensity factor is given by $K = \sigma\sqrt{\pi c}$ where σ is the applied stress. Substituting these quantities to Eq.(8), the following relation is obtained;

$$\frac{dc}{dN} \sim \Delta\sigma^m c^{m/2} \quad (9)$$

where $\Delta\sigma$ is the difference between the minimum and maximum applied stresses.

As mentioned above, the particle cluster periodically passes the principal axes of the fluid stress tensor owing to its rotation. Therefore we can consider the particle cluster in shear flow is exposed to the cyclic stress $\sigma_{\min,\max} = \pm\mu\dot{\gamma}$ for a period $\dot{\gamma}t = 4\pi$. If the interparticle force is constant, $\Delta\sigma$ is directly proportional to Fa . Since $-(k - k_S)$ can be interpreted as the amount (length) of the flaw c , Eq.(7) is similar to Eq.(9) with $m = 2$ or $m = 2.5$. We concluded that the long-term structural change of dense particle clusters might be explained by the analogy of the fatigue crack growth in the cluster.

In most of the previous studies on the breakup of the particle cluster in fluid flow, it has been explained that the breakup process is dominated by an static balance between the cohesive strength of the cluster and the fluid stress. Although our calculation system is somewhat far from the actual system, *i.e.*, less primary particles, no consideration of penetration effect, *etc.*, the obtained results suggest the breakup behavior of the particle clusters should be considered as the dynamic one.

Conclusions

The long-term structural change of a dense particle cluster in shear flow has been investigated numerically. The simulation results indicate that the both rotation and strain effects of shear flow bring about the restructuring of the particle cluster. The change in the structure shows similarities if any fluid stress is applied and is explained as the initial rearrangement of primary particles and the successive crack growth that takes a long time. The crack growth in the cluster is similar to that of the solid materials under cyclic load and could be explained by the analogy of the fracture mechanics.

References

- [1] Y. Xia, B. Gates, Y. Yin and Y. Lu, *Adv. Mater.* 12 (2000) 693.
- [2] J. L. Ottino, P. DeRoussel, S. Hansen, D. V. Khakhar, *Adv. Chem. Eng.* 25 (2000) 105.
- [3] P. Taboada-Serrano, C.-J. Chin, S. Yiacoumi, C. Tsouris, *Curr. Opin. Colloid Int. Sci.* 10 (2005) 123.
- [4] I. Y. Z. Zia, R. G. Cox and S. G. Mason, *Proc. Roy. Soc. A.* 300 (1967) 421.
- [5] C. M. Schroeder, R. E. Teixeira, E. S. G. Shaqfeh and S. Chu, *Phys. Rev. Lett.* 95 (2005) 018301.
- [6] M. Y. Lin, R. Klein, H. M. Lindsay, D. A. Weitz, R. C. Ball, P. Meakin, *J. Colloid Int. Sci.* 137 (1990) 263.
- [7] V. Oles, *J. Colloid Interface Sci.* 154 (1992) 351.
- [8] T. Serra and X. Casamitjana, *J. Colloid Int. Sci.* 206 (1998) 505.
- [9] S. Harada, R. Tanaka, H. Nogami and M. Sawada, *J. Colloid Int. Sci.* 301 (2006) 123.
- [10] M. Doi and D. Chen, *J. Chem. Phys.* 90 (1989) 5271.
- [11] K. Higashitani, K. Imura, H. Sanda, *Chem. Eng. Sci.* 56 (2001) 2927.
- [12] M. Fanelli, D. L. Feke, I. Manas-Zloczower, *Chem. Eng. Sci.* 61 (2006) 473.
- [13] J. F. Brady, G. Bossis, *Ann. Rev. Fluid Mech.* 20 (1988) 111.
- [14] L. Durlofsky, J. F. Brady, G. Bossis, *J. Fluid Mech.* 180 (1987) 21.
- [15] S. Kim, S. J. Karrila, *Microhydrodynamics*, Butterworth-Heinemann, Boston, (1991).
- [16] D. J. Jeffery, Y. Onishi, *J. Fluid Mech.* 139 (1984) 261.
- [17] H. C. Hamaker, *Physica* 4 (1937) 1058.
- [18] W. R. Bowen, F. Jenner, *Adv. Colloid Int. Sci.* 56 (1995) 201.
- [19] J. N. Israelachvili, *Intermolecular and Surface Forces*, Academic Press, London, (1992).
- [20] N. Yu, A. A. Polycarpou, *J. Colloid Int. Sci.* 278 (2004) 428.
- [21] H. Rumpf, *Chem. Ing. Tech.* 30 (1958) 144.
- [22] K. Kendall, *Powder Metallurgy* 31 (1988) 28.
- [23] F. Ellyin, *Fatigue Damage, Crack Growth and Life Prediction*, Chapman and Hall, London, (1997).

Fig.1 Schematic diagram of calculation system and initial configuration of particle cluster

Fig.2 Instantaneous motion of particle cluster on x - y plane in steps of normalized time $\dot{\gamma}t = 200$ for flow condition $\mu\dot{\gamma} = 23.9\text{Pa}$

Fig.3 Average coordination number of primary particle before rupture for $\mu\dot{\gamma} = 23.9\text{Pa}$

Fig.4 Average coordination number of primary particle before rupture for various $\mu\dot{\gamma}$

Fig.5 Average coordination number of primary particle in clusters having different structures (solid line: $k_0 = 5.54$, dashed line: $k_0 = 5.04$)

Fig.6 Relation between nondimensional time $Fa^{2.5}\dot{\gamma}t$ and average coordination number $k - k_s$

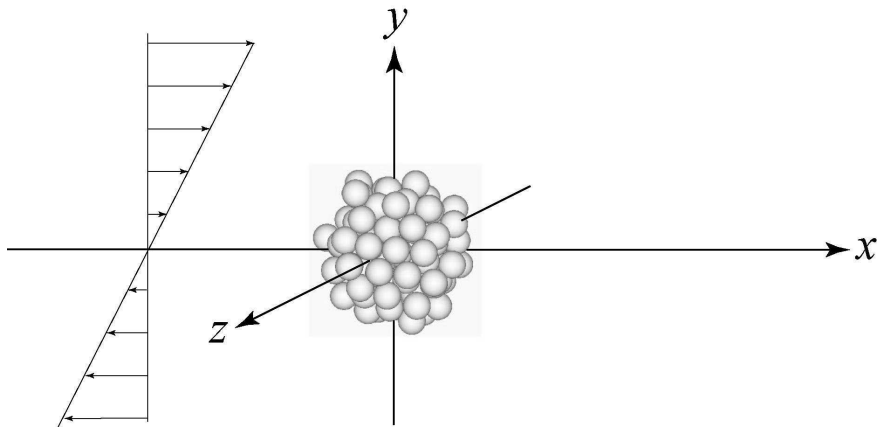


Fig.1 Schematic diagram of calculation system and initial configuration of particle cluster

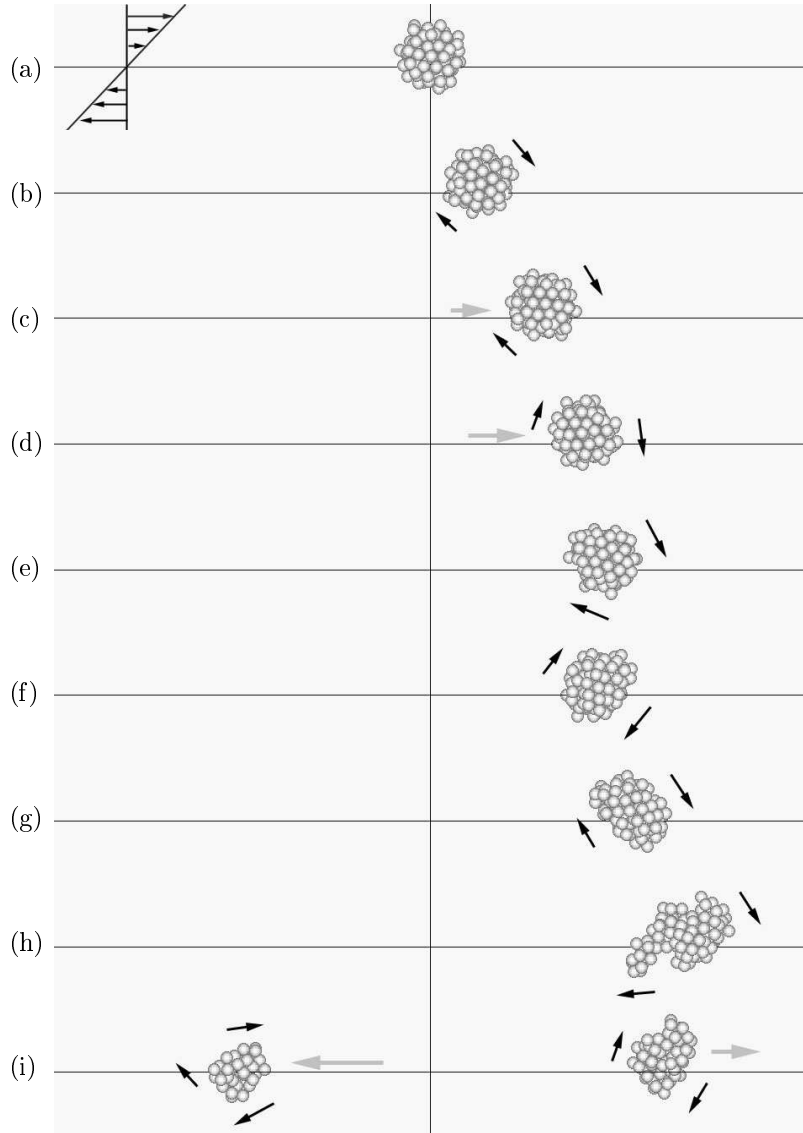


Fig.2 Instantaneous motion of particle cluster on x - y plane in steps of normalized time $\dot{\gamma}t = 200$ for flow condition $\mu\dot{\gamma} = 23.9\text{Pa}$

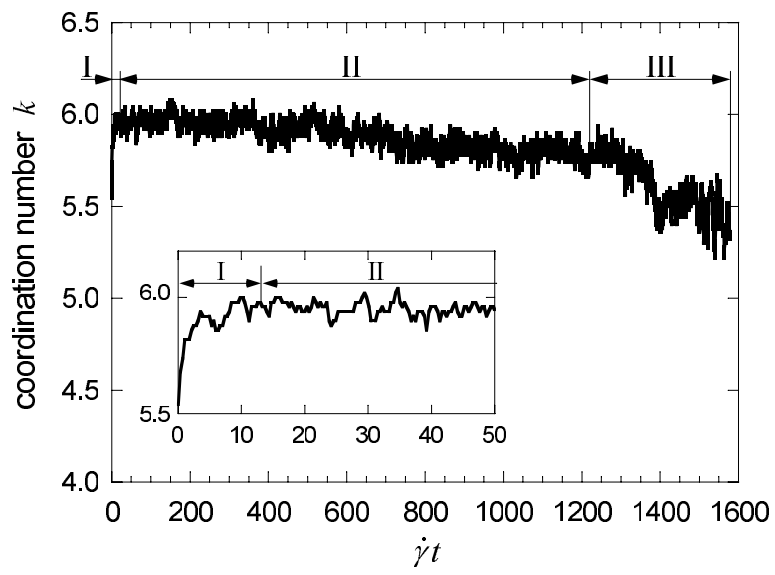


Fig.3 Average coordination number of primary particle before rupture for $\mu\dot{\gamma} = 23.9\text{Pa}$

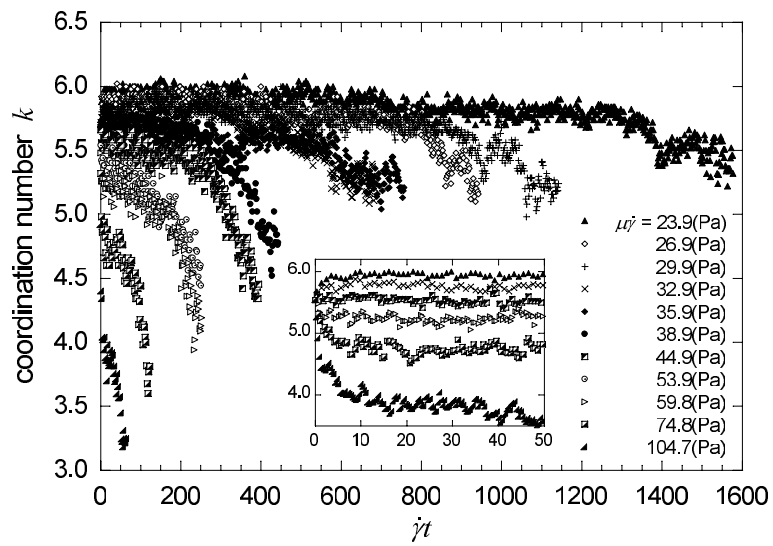


Fig.4 Average coordination number of primary particle before rupture for various $\mu\dot{\gamma}$

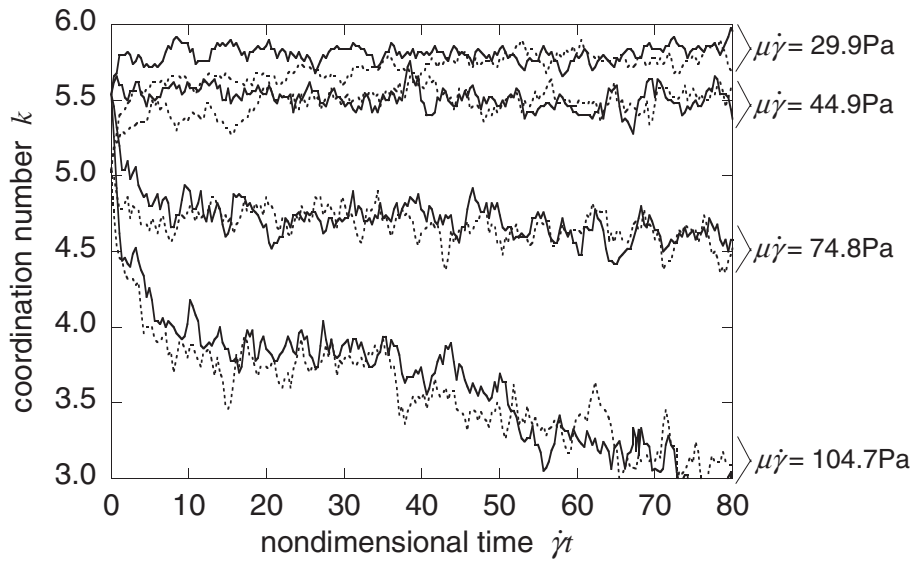


Fig.5 Average coordination number of primary particle in clusters having different structures (solid line: $k_0 = 5.54$, dashed line: $k_0 = 5.04$)

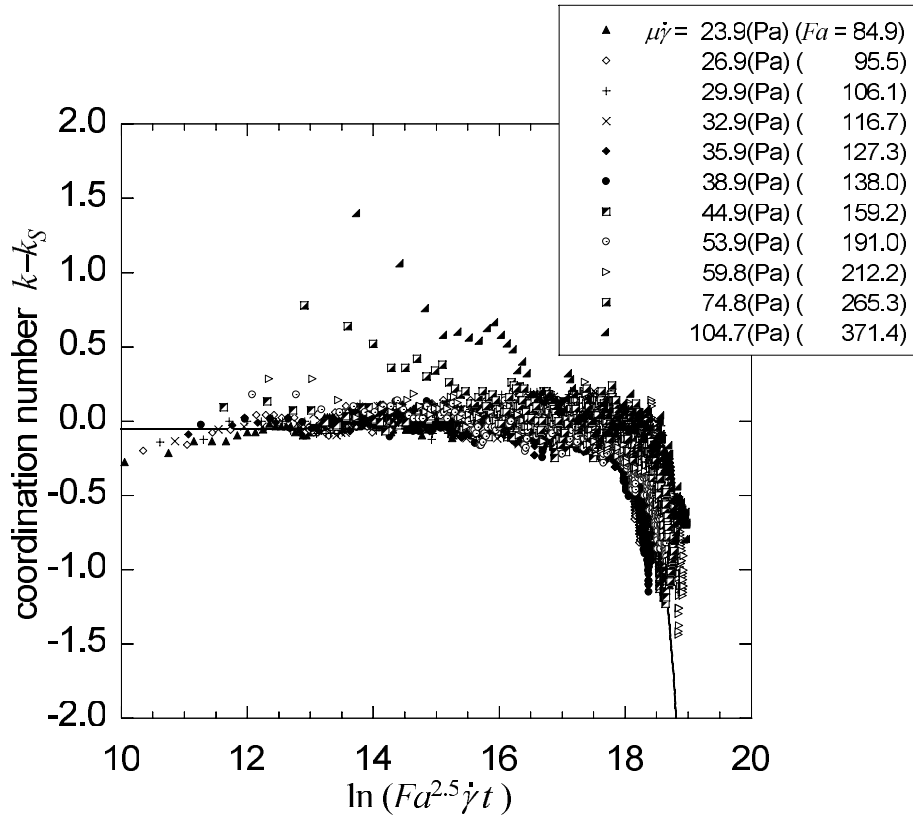


Fig.6 Relation between nondimensional time $Fa^{2.5}\dot{\gamma}t$ and average coordination number $k - k_S$